Pergamon

Int. J. Heat Mass Transfer. Vol. 39, No. 15, pp. 3211–3220, 1996

0017-9310/96 $15.00 + 0.00

0017-9310(95)00409-2

Heat transfer and pressure drop characteristics of ten radiator tubes

C.-O. OLSSON

Chalmers University of Technology, Department of Thermo and Fluid Dynamics, 412 96 Göteborg, Sweden

and

B. SUNDÉN†

Lund Institute of Technology, Division of Heat Transfer, Box 118, 221 00 Lund, Sweden

(*Received* 3 *November* 1994 *and in final form* 13 *October* 1995)

Abstract—The thermal and hydraulic performance of ten radiator tubes has been investigated. The tubes tested are one smooth tube, two rib-roughened tubes, five dimpled tubes and two offset strip fin tubes. The tubes are representative of flat tube geometries applied in automotive heat exchangers, for example radiators. Isothermal pressure drop data were taken for Reynolds numbers in the range of 500–6000. These data are presented as Fanning friction factors and inlet loss coefficients. Heat transfer data were taken in the same Reynolds number range and the results are presented as Colburn j factors, as well as Nusselt numbers. The tubes are compared by considering the flow area goodness factor and the volume goodness factor. The rib-roughened tubes showed the best performance. The offset strip fin tube results could be correlated within 20% by correlations available in the literature. For all tubes, simple correlations of the results are provided. Copyright © 1996 Elsevier Science Ltd.

INTRODUCTION

To improve the heat transfer from a surface, it is common to apply turbulence promoters or roughness elements to the surface. In radiators, which are vital components in the control of the engine temperature in cars, trucks and buses, a liquid (commonly a water–glycol mixture) is to be cooled by air. The liquid flows in flat tubes while the air flows in channels set up by multilouvered fin surfaces. In many situations the thermal resistance on the air side is larger than that on the liquid side. Thus, the performance of louvered surfaces has been investigated extensively, see e.g. refs. [1–4]. However, in some situations and for optimal design, also the performance of liquid tubes needs careful consideration and improvement. The flat tubes on the liquid side are generally of small dimensions, and to enhance the heat transfer process ribs or dimples are rolled into two opposite walls. Inserts (or turbulators) like offset strip fins are employed particularly for oil coolers.

Publications on the heat transfer and pressure drop characteristics of real radiator tubes are rare, and the only papers known to the authors are those of Farrell *et al.* [5] and Olsson and Sundén [6]. In these reports, Nusselt numbers, j-factors, and f-factors were presented for some radiator tubes. On the other hand, idealized and laboratory manufactured rectangular channels with roughness elements on two opposite walls have been investigated. Particularly many papers, both experimental and numerical ones, on rib-roughened surfaces have been published. Correlations have been developed for the friction factors and the j-factor based on experimental data. Recent papers are those of Chang and Mills [7], Zhang *et al.* [8], and Liou and Hwang [9]. More general reviews of enhanced heat transfer surfaces have been presented by Webb [10, 11].

The present paper concerns an experimental investigation of the thermal and hydraulic performance of 10 real radiator tubes. It is a continuation and an extension of the work in Olsson and Sundén [6]. Additional radiator tubes have been investigated, correlations have been developed and the discussion and the physical interpretation of the results are extended considerably.

EXPERIMENTAL ARRANGEMENT

The dimensions of the tubes tested are listed in Table 1, and a photograph of the outside top surfaces of all tubes except for the offset strip fin tubes is shown in Fig. 1. The smooth and rib-roughened tubes are made of brass, while the dimpled and offset strip fin tubes are made of aluminium. The roughness elements on the outside bottom surfaces of the tubes pictured

† Author to whom correspondence should be addressed.

NOMENCLATURE

A	heat transfer area
A	constant in correlation
A_c	tube cross sectional area
B	constant in correlation
C	constant in correlation
c_p	specific heat
D	constant in correlation
D_h	hydraulic diameter
e	roughness height
E	pumping power per unit heat transfer area
f	Fanning friction factor
h	height of the offset strip fin channel
H	tube height
j	Colburn heat transfer factor ($=StPr^{2/3}$)
K_c	inlet loss coefficient
l	length of fin
L	tube length
Nu	average Nusselt number ($=\alpha D_h/\lambda$)
p	rib spacing
Pr	Prandtl number
R	residual of curve fit
Re	Reynolds number ($=u_m D_h/\nu$)
s	lateral fin spacing
St	Stanton number ($=Nu/RePr$)
t	fin thickness and wall thickness
T	temperature
u_m	mean velocity
W	tube width
x	coordinate in the main flow direction.

Greek symbols

α	heat transfer coefficient
α	aspect ratio s/h
γ	ratio t/s
δ	ratio t/l
Δp	pressure drop
η	ratio $(j/j_s)/(f/f_s)$
θ	angle of attack to flow
λ	thermal conductivity
ν	kinematic viscosity
ρ	density.

Subscripts

fd	refers to fully developed conditions
in	at the tube inlet
out	at the tube outlet
s	for the smooth tube
wall	at the tube wall.

in Fig. 1 are staggered in the streamwise direction and, for the dimpled tubes, also in the lateral direction. The smooth tube has an approximately rectangular cross-section with a hydraulic diameter, D_h, of 3.11 mm and an aspect ratio of 8.3. The rib-roughened tubes have aspect ratios 8.4 (r1) and 13.2 (r2), and parallel ribs are rolled into the opposite wide walls. The rib spacing, p, and the angle of attack to the flow, θ, are the same for both tubes while the rib height, e, is slightly larger for r2 than for r1. The angle of attack to the flow is defined as zero for ribs perpendicular to the flow direction.

The dimpled tube d1 has an aspect ratio of 7.6 and two rows of dimples are rolled into the wide walls with a lateral spacing of 4.1 mm and a streamwise spacing, p, of 4.5 mm. The dimpled tubes d2 and d3 have three rows of dimples on one wall and four rows on the other, d4 has four vs five, and d5 has five vs five rows. The dimple height is the same, but the relative height e/H is largest for d2 and smallest for d1.

A typical offset strip fin geometry is shown in Fig. 2. The tubes tested have identical insert geometries as is seen from Table 1. The only difference is the width of the tubes, i.e. the number of flow passages in each cross-section of the tubes are different, osf1 having seven and osf2 having 11 flow passages. The offset

Table 1. Dimensions of tubes tested

Tube	D_h [mm]	A_c [mm^2]	p [mm]	e [mm]	H [mm]	W [mm]	θ [deg]	t [mm]
Smooth (s)	3.11	25.3		-	1.74	14.5	—	0.18
Rib-roughened (r1)	3.11	25.4	4.0	0.18	1.74	14.6	30	0.18
Rib-roughened (r2)	3.05	35.4	4.0	0.20	1.64	21.6	30	0.18
Dimpled (d1)	3.53	30.4	4.5	0.45	2.00	15.2	30	0.35
Dimpled (d2)	2.81	27.8	4.8	0.45	1.52	18.3	18	0.35
Dimpled (d3)	3.08	38.4	4.8	0.45	1.65	23.2	18	0.35
Dimpled (d4)	3.08	38.4	4.8	0.45	1.65	23.2	18	0.35
Dimpled (d5)	3.08	38.4	4.8	0.45	1.65	23.2	18	0.35

Offset strip fin tubes	D_h [mm]	A_c [mm^2]	h [mm]	s [mm]	l [mm]	H [mm]	W [mm]	t [mm]
(osf1)	2.82	64.2	2.6	3.5	5.0	3.0	26.2	0.4
(osf2)	2.82	111	2.6	3.5	5.0	3.1	43.4	0.4

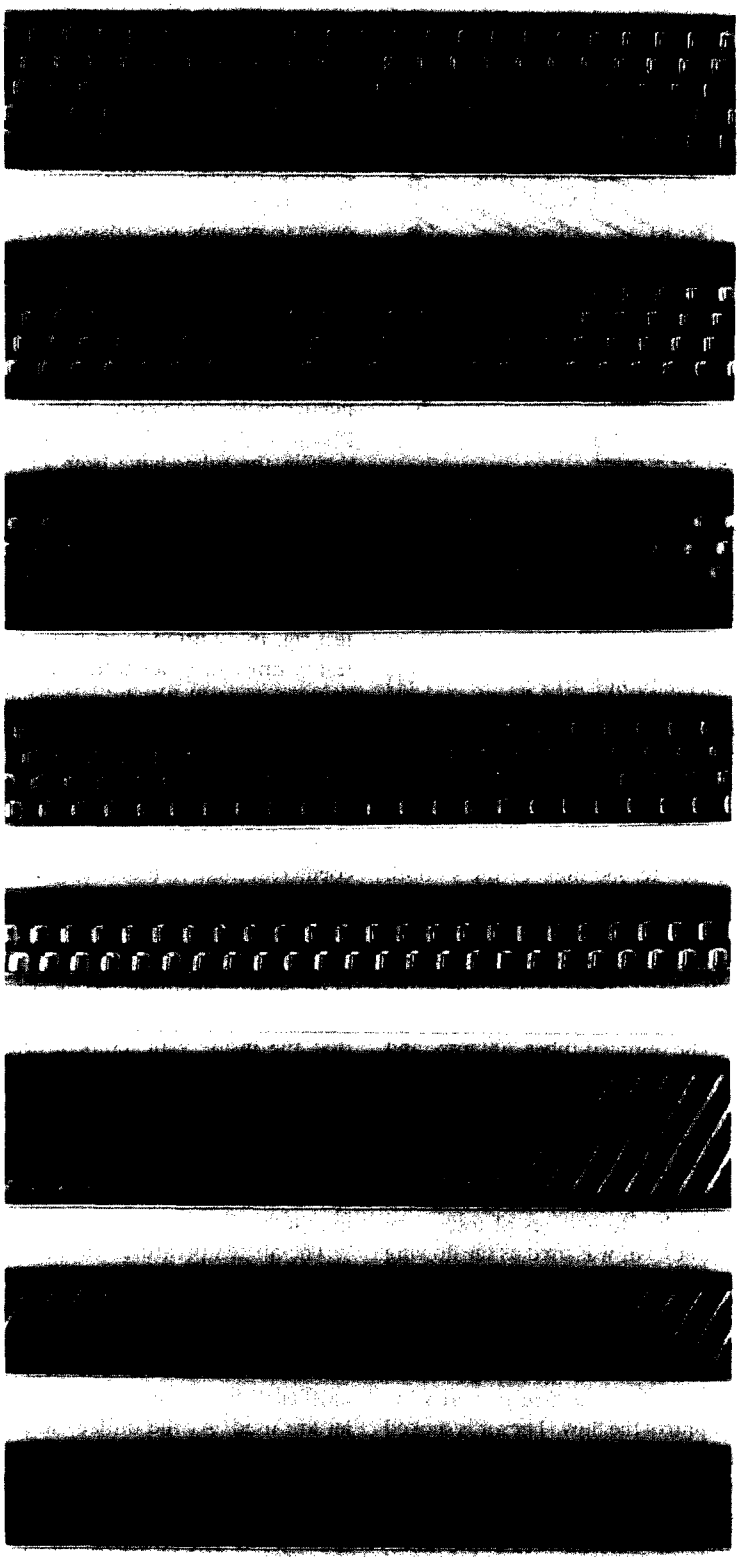

Fig. 1. Outside top surfaces of the tubes tested. From the left: s, r1, r2, d1, d2, d3, d4 and d5.

strip fin tubes are carefully cut out from complete oil coolers. The inserts have been soldered to the inner tube surface using the non-corrosive locking (Nocoloc) method. The geometry of the insert can also be expressed in the dimensionless parameters α, δ and γ, where $\alpha = s/h = 1.35$, $\delta = t/l = 0.080$, and $\gamma = t/s = 0.114$. The hydraulic diameter has been determined according to Manglik and Bergles [12] as

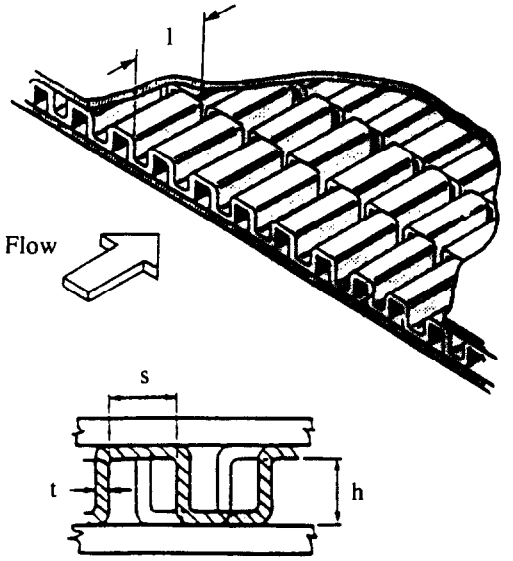

Fig. 2. Offset strip fin geometry (from Manglik and Bergles [12]).

$$D_h = 4shl/[2(sl+hl+th)+ts] \quad (1)$$

where the blunt edges ($2th$ and ts) are accounted for. Equation (1) has been chosen since the results will be compared to correlations by Manglik and Bergles [12].

In the pressure drop tests the effect of the inlet is described by K_c, and in the heat transfer tests the tube length is varied from 100 to 350 mm for the smooth tube and for the rib-roughened tube $r1$ to enable determination of the required tube length to achieve negligible influence of the tube length on the average heat transfer coefficient. When all tubes are compared, the lengths are: for the smooth tube 350 mm, for the rib-roughened tubes and the dimpled tubes 200 mm, and for the offset strip fin tubes 150 mm. Very long tubes can not be used because the temperature difference between the bulk of the fluid and the wall at the outlet must be measurable with sufficient accuracy.

The pressure drop and heat transfer investigations were performed separately. Both series of tests were carried out on single tubes. Air was used as the flowing medium in both tests, and the pressure drop measurements were performed at isothermal conditions. The pressure drop test rig consists of a fan, two rotameters to measure the flow rate (Krohne, flow ranges 0.12–1.2 $m^3 h^{-1}$ and 1.2–8 $m^3 h^{-1}$, respectively), and a bypass arrangement to control the flow. The air is sucked into the tested tube from the quiescent room. To enable pressure drop measurements the tubes are equipped with pressure taps with a hole diameter of 0.5 mm. No visible burr has been allowed at the holes, and short 1 mm diameter stainless steel tubes have been glued on top of the holes as connections for flexible tubes. This arrangement provides openings which are flush with the inner tube wall. However, a secondary flow is present in the tubes which may influence the pressure at each hole.

The smooth tube, the rib-roughened tubes, and the dimpled tubes have 10 pressure taps each. The pressure taps are placed at one of the short sides with a spacing of approximately 20 hydraulic diameters in the streamwise direction. For the offset strip fin tube the pressure is measured at four cross-sections with a spacing of approximately 20 hydraulic diameters. At each cross-section three pressure taps are installed in order to provide the cross-sectional average pressure. This is necessary since the pressure may vary in a cross-section due to imperfections in the symmetry. Some of the tubes have a wall thickness of only 0.18 mm, and special care has been taken when instrumenting these tubes. The inlets of the tubes are suspended with no nearby surfaces and at atmospheric pressure, and no effects of distortion due to low pressure in the tubes have been observed. The pressure drops are measured with a micromanometer, FCO14 Furness Controls Ltd, and the signals are recorded by a Macintosh II using a MacADIOS card.

The heat transfer test rig consists of a fan and the same flow rate control system as in the pressure drop test rig. In addition there is a heater upstream of the tested tube. In order to obtain constant temperature at the tube wall, the tube is mounted on a so-called water table. Water is flowing around the tube in cross flow with a speed of approximately 1 m s^{-1}, and a two-dimensional contraction is placed upstream of the tube to make the water flow uniform. This provides the outer tube wall with a heat transfer coefficient that is much larger than the inside wall heat transfer coefficient. The thermal resistance on the outer side is thus much less than that on the inside of the tube and is assumed negligible. Under the prevailing circumstances the thermal resistance in the tube wall is also negligible. It can therefore be assumed that the inside wall temperature is the same as the temperature of the water. Since the water flow rate is high and the heat flux modest, the water temperature is considered as constant and uniform. The temperature difference at the inlet is approximately 70°C and the temperature difference at the outlet is 1–10°C, depending on the flow rate.

The air temperatures are measured using 0.25 mm copper–constantan thermocouples, and the voltages are recorded by a Keithley 199 System DMM/Scanner. At the tube inlet and outlet two thermocouples are used. In the determination of the heat transfer coefficient the mean temperatures at the inlet and outlet are used. At the outlet there is a large difference between the maximum and the minimum temperature. To obtain the outlet bulk temperature the tube outlet is connected to an insulated enclosure where mixing takes place. The air leaves the enclosure through two circular holes in which the thermocouples are placed.

An additional thermocouple is used to measure the temperature at the flow meter. The water temperature is taken by a mercury thermometer. At the heat transfer rig no pressure drop measurements are carried out. Only the pressures after the tube and at the flow meter are taken so that the densities can be calculated.

DATA EVALUATION

The pressure drop data are presented in terms of the Fanning friction factor, f, and the inlet loss coefficient, K_c. These parameters are determined from the non-dimensional pressure drop equation, see e.g. Kakaç *et al.* [13] and Eckert and Drake [14],

$$\frac{\Delta p}{\rho u_m^2/2} = K_c + (fRe)_{fd}\frac{4x}{D_h Re} \tag{2}$$

by performing a least squares fit of a line to the straight part of the plot of $\Delta p/(\rho u_m^2/2)$ vs $x/(D_h Re)$. The slope is equal to $4(fRe)_{fd}$, and the intercept is equal to K_c. K_c includes everything not being the fully developed friction factor. However, the various contributions to K_c were not possible to separate out. The velocity u_m is the mean velocity calculated from the mass flow rate divided by the density and cross-sectional area of the tube. The cross-sectional area of the offset strip fin tube is taken as the cross-sectional area of the tube itself minus the cross-sectional area of the insert. For the rib-roughened and the dimpled tubes the cross-sectional area is measured at the base of the roughness elements. The Reynolds number is determined from

$$Re = \frac{u_m D_h}{\nu}. \tag{3}$$

The pressure at the inlet, $x = 0$, is taken as the air pressure outside the tube. This means that the inlet loss coefficient includes the acceleration of the fluid from rest. A term of value unity is thus added to K_c as compared to the entrance pressure-loss coefficients presented in, e.g. Kays [15] and Kays and London [16].

The heat transfer data are presented as Colburn heat transfer factor, j, vs Reynolds number. The j factor is defined as

$$j = StPr^{2/3} = \frac{\alpha}{c_p \rho u_m} Pr^{2/3} = \frac{Nu}{RePr^{1/3}}. \tag{4}$$

The fluid properties are determined from the mean values of temperature and pressure upstream and downstream of the tube. The heat transfer coefficient is obtained as

$$\alpha = \frac{\rho u_m A_c c_p}{A} \ln\left|\frac{T_{in} - T_{wall}}{T_{out} - T_{wall}}\right| \tag{5}$$

where A_c is the cross-sectional area and A the heat transfer area. The ratio of these areas can be expressed as

$$\frac{A_c}{A} = \frac{D_h}{4L} \tag{6}$$

where L is the length of the tube.

Different methods have been proposed for assessment and comparison of the performance of various heat transfer surfaces. These have been summarized and reviewed by Shah [17]. Recently, a family of comparison methods was presented by Cowell [18]. Relative values of five parameters were used and it was shown how these values are derived and how comparisons can be made. In this paper the so-called flow area goodness factor and the volume goodness factor are considered. The flow area goodness factor presents j/f vs Reynolds number, and the higher the j/f factor is, the greater the heat transfer per unit pressure drop will be. The volume goodness factor represents a plot of the heat transfer coefficient (α, W m^{-2} K^{-1}) vs the pumping power per unit heat transfer area (E, W m^{-2}). A high position in such a graph indicates an efficient heat transfer surface. α and E can be expressed as

$$\alpha = \frac{jRe\lambda Pr^{1/3}}{D_h} \tag{7}$$

$$E = \frac{fRe^3 \rho \nu^3}{2D_h^3}. \tag{8}$$

To judge the overall advantage of enhanced surfaces, savings in material and packaging costs vs added manufacturing costs and pumping power requirements also have to be considered.

ESTIMATION OF UNCERTAINTY

For the components in the pressure drop test rig the following uncertainties have been estimated. The micromanometer has been calibrated to give a maximum error of less than $\pm 1\%$. An important contribution to the pressure drop uncertainty is the error due to the scatter in the pressure drop data for each least squares fit. This scatter is due to uncontrolled parameters such as the exact shape of the pressure tap holes, secondary flows, etc. The maximum errors in the intercept K_c and the slope $(4fRe)_{fd}$ have been estimated with the maximum likelihood method and 95% confidence to be within $\pm 5\%$, see e.g. Box *et al.* [19].

The thermocouples used in the heat transfer test rig are calibrated individually, and the maximum error is estimated to be ± 0.05°C. This estimate also holds for the mercury thermometer used for measuring the water temperature. The inlet air temperature controlled by the heater varies up to ± 0.5°C.

The rotameters have been calibrated and the error is less than $\pm 1\%$. Corrections are also made to allow for changes in temperature and pressure during the tests. The geometric quantities of the tubes have been determined within ± 0.05 mm.

A root-sum-square combination of the effects of each of the individual sources of error (see e.g. Moffat [20]) yields the following estimates of the uncertainties: $f \pm 8\%$, $K_c \pm 11\%$, $Re \pm 4.5\%$, $Nu \pm 8\%$, $j \pm 9\%$. In general, the measurements are shown to be reproducible well within these limits. However, it has not been possible to estimate the deviation between the measured outlet temperature and the true outlet

bulk temperature. This problem may therefore give rise to an additional error in the heat transfer data.

The error in the Nusselt number, due to finite values of the thermal resistances of heat conduction in the tube wall and forced convection on the outer side of the tube, is estimated to be less than -1% for laminar flow. For the highest flow rates this error is less than -5%. The negative sign means that the true values are greater than the measured and reported ones. There may also be an underestimating of the Nusselt number due to the sealings at the tube ends. The sealings cover less than 5 mm of each tube end, which for a 200 mm long tube may give an error less than 5%.

The fin efficiency of the offset strip fins has been found to be unity. Thus, the fins do not introduce a thermal resistance. The Nocoloc bonding method may introduce a thermal resistance between the fins and the tube walls. However, no estimation of this resistance has been possible, but in case it exists, it is included in the presented heat transfer coefficients.

RESULTS AND DISCUSSION

The measurements were carried out in the Reynolds number range $500 < Re < 6000$. The pressure drop data, the heat transfer data, and the performance comparison are discussed separately.

Pressure drop data

Figure 3 shows the friction factor vs the Reynolds number for all the tubes (except for osf2). As may be expected, the smooth tube exhibits the lowest friction factor. The slope in the laminar region corresponds to $fRe = 17.7$, which is lower than the value predicted for laminar flow in a rectangular tube with an aspect ratio of 8.3. According to Shah and London [21] $fRe = 20.7$. The difference is probably due to effects of the rounded corners in the radiator tube. At the highest Reynolds numbers the data agree with the Blasius relation (Kakaç *et al.*[13]):

$$f = 0.0791 Re^{-0.25} \tag{9}$$

while at lower Reynolds numbers the smooth tube data is somewhat lower. At $Re = 5000$ the measurements are 11% lower than predicted by the Balsius relation.

In a previous paper, [22], we have reported the friction factors of small-sized smooth circular and rectangular channels. The measuring and evaluation procedures were quite similar to those in this paper. The results for both laminar and turbulent flow agreed very well with the values reported in the literature.

All the other tubes show significantly larger friction factors at both laminar and turbulent flow. At laminar flow the f factor curves of the augmented tubes will never reach the smooth tube curve, since the surface modifications make the true cross-sectional area less than the calculated one and hence, the true mean velocity is higher than the calculated velocity. The rib-roughened tubes have almost identical f factors at turbulent flow while at laminar flow f for r2 is higher than f for r1. This latter fact is likely due to the difference in aspect ratio. The dimpled tubes d1, d4 and d5 show almost equal f factors. The tube d2 has a higher f factor than the other dimpled tubes which is due to the comparatively large ratio e/H, which creates a larger flow resistance. The tube d3 has a slightly lower f factor than d4 and d5, which have the same tube dimensions. The reason is that tube d3 has less dimples which leaves more undisturbed area in the cross-section, and thus the flow resistance is smaller. The difference between osf1 and osf2 is very small in both the f and the j factor, and therefore only osf1 is included in the figures. The f factor of osf1 is higher than all other tubes except for d2.

Figure 4 shows the inlet loss coefficient K_c vs the Reynolds number. The general behaviour of the inlet loss coefficient is that it decreases with increasing Reynolds number at turbulent flow. At low Reynolds numbers it is impossible to measure the inlet loss coefficient accurately because it is dominated by the separation and reattachment of the flow close to the inlet. This flow field is very sensitive to small defects in the geometry and to disturbances in the upstream flow. By analyzing the curves for d3, d4 and d5 it is found that K_c decreases with increasing roughness (or number of dimples), and from the curves for r1 and

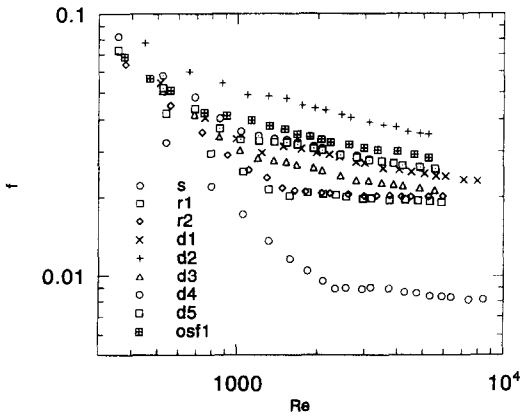

Fig. 3. Fanning friction factor vs Reynolds number.

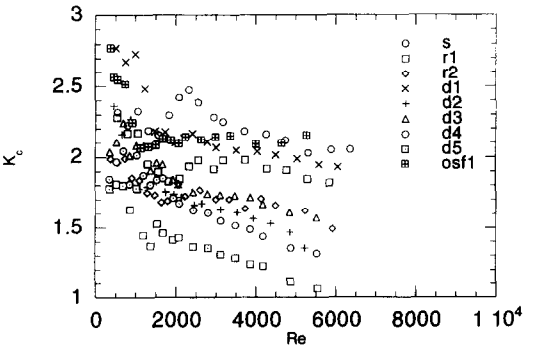

Fig. 4. Inlet loss coefficient vs Reynolds number.

r2 it is found that K_c decreases with increasing aspect ratio. It is expected that the smooth tube exhibits the largest inlet loss coefficient, since the entrance region extends further in a smooth tube than in a rough tube. Detailed measurements of the inlet loss coefficient for smooth circular and rectangular tubes are reported in Olsson and Sundén [22]. It is found that at turbulent flow K_c varies from 1.2 to 1.6, depending on the tube size. Thus, the radiator tubes in this investigation provide larger inlet loss coefficients than the smooth tubes of the earlier investigation.

Heat transfer data

Figure 5 shows the average Nusselt number for the smooth tube. The tube length is varied from 100 to 350 mm and it is obvious that the tube length influence on the Nusselt number is more pronounced in laminar flow than in turbulent flow. A correlation of Nu as a function of Re and L/D_h, where L is the tube length, has been determined for $3000 < Re < 6000$. It reads

$$Nu = ARe^B \tag{10}$$

where

$$A = 28.4(L/D_h)^{-1.60} \tag{11}$$

$$B = 0.308(L/D_h)^{0.211}. \tag{12}$$

The correlation is valid for $30 < L/D_h < 120$. Since only one smooth tube geometry was considered it was not possible to include the aspect ratio in equations (10)–(12).

Figure 6 shows the Nusselt number for the rib-roughened tube r1. The influence of the entrance region is only seen for the shortest tubes with $L = 100$ and 150 mm. Among the longer tubes the difference in Nu is negligible. Hence, it is believed that heat transfer data obtained as average values for a tube of 200 mm length is representative for fully developed thermal conditions.

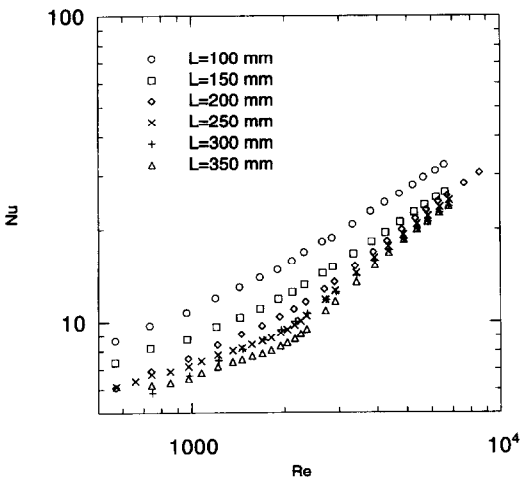

Fig. 5. Nusselt number vs Reynolds number for smooth tubes of different lengths.

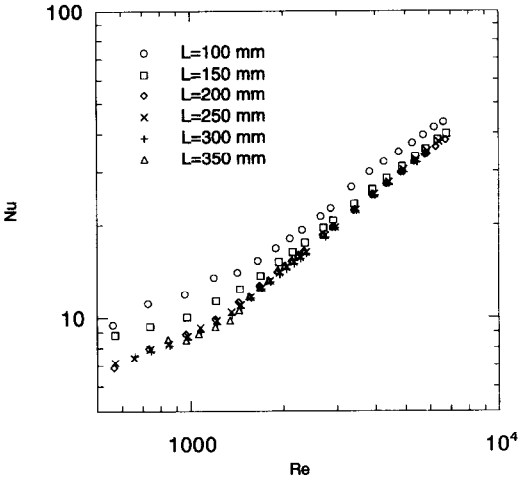

Fig. 6. Nusselt number vs Reynolds number for rib-roughened tubes, r1, of different lengths.

The heat transfer data for all the tubes are presented as the j factor vs the Reynolds number in Fig. 7. The smooth tube provides the lowest j factor, while all the other tubes show significantly higher j factors. The smooth tube slope in the laminar region corresponds to a Nusselt number equal to 6.5, which is higher than the theoretical value, 5.65, for a rectangular tube with the same aspect ratio, cf. Shah and London [21]. For turbulent flow the heat transfer data are well correlated by the Gnielinski correlation (Kakaç *et al.* [13])

$$Nu = \frac{(f/2)(Re-1000)Pr}{1+12.7(f/2)^{1/2}(Pr^{2/3}-1)}. \tag{13}$$

All the enhanced tubes have better heat transfer performance than the smooth tube. However, the difference in performance between the enhanced tubes is less than 20%. At Reynolds numbers 1000–2000, the rib-roughened tubes have slightly lower j factors

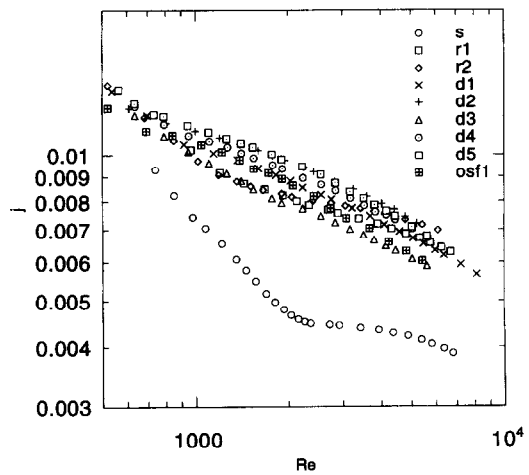

Fig. 7. Average Colburn factor vs Reynolds number.

Table 2. Performance comparison at $Re = 5000$ (osf2 at $Re = 3000$)

Tube	f/f_s	j/j_s	j/f	η
Smooth (s)	1	1	0.502	1
Rib-roughened (r1)	2.32	1.63	0.352	0.702
Rib-roughened (r2)	2.42	1.74	0.361	0.720
Dimpled (d1)	2.93	1.61	0.275	0.549
Dimpled (d2)	4.19	1.74	0.209	0.416
Dimpled (d3)	2.58	1.46	0.284	0.565
Dimpled (d4)	3.09	1.67	0.271	0.541
Dimpled (d5)	3.10	1.69	0.274	0.546
Offset strip fin (osf1)	3.41	1.48	0.217	0.433
Offset strip fin (osf2)	3.50	1.60	0.230	0.459

than the dimpled tubes (except for d3) and the offset strip fin tube, but at higher Reynolds numbers the difference vanishes.

For each tube a simple power series correlation has been fitted to the friction factor ($4fRe$) and another one to the heat transfer data (Nu). These correlations are presented in Table 3. The residuals are reported for all cases. If one assumes that the Nusselt number is proportional to $Pr^{1/3}$, the correlations should be applicable to other fluids if the calculated Nusselt numbers are multiplied by the Prandtl number ratio to the power one third.

The correlations for the dimpled tube d2 have been compared with data from measurements on a full-scale radiator, see Olsson and Sundén [23]. The friction factor and the j-factor was predicted within $\pm 4\%$ and $\pm 10\%$, respectively.

Performance comparison

The performance of all tubes are compared in Table 2 at $Re = 5000$. The ratios f/f_s, j/j_s, j/f, and the efficiency $\eta = (j/j_s)/(f/f_s)$ are provided. The higher η, the greater is the heat transfer improvement per unit pressure drop increase. The rib-roughened tubes show the greatest heat transfer enhancement per unit pressure drop increase. However, to achieve a 74% increase in j, the friction factor is increased by a factor 2.42. The dimpled tube d2 provides the same increase in the j-factor as the rib-roughened tube r2, but at a much higher pressure drop penalty. In the Reynolds number range investigated, η decreases slightly with increasing Re for all the tubes.

Farrell *et al.* [5] investigated the heat transfer characteristics of four radiator tubes (one smooth) and the friction factor of seven tubes. The efficiency η was generally lower than reported here.

The volume goodness factors are presented in Fig. 8. The diagram shows the heat transfer coefficient vs the pumping power per unit heat transfer area. The curve-fitted expressions in Table 3 were used as Fig. 8 was constructed. The rib-roughened tubes provide the highest positions and thus seem to be the most efficient ones. The dimpled tubes show a slightly better performance than the offset strip fin tube, while the smooth tube curve takes the lowest position. A word

Table 3. Curve fit expressions for the presented data. The expressions are valid at $500 < Re < 6000$ (osf2 $500 < Re < 4000$)

Tube	A	B	C	D	R
		Pressure drop data curve fit $4(fRe) = A + BRe + C(Re)^2 + D(Re)^3$			
Smooth (s)	68.820	-6.6978×10^{-3}	7.7586×10^{-6}	-4.9240×10^{-10}	0.99837
Rib-roughened (r1)	68.481	2.0923×10^{-2}	1.5890×10^{-5}	-1.4555×10^{-9}	0.99939
Rib-roughened (r2)	90.906	1.7260×10^{-3}	2.1242×10^{-5}	-1.7957×10^{-9}	0.99951
Dimpled (d1)	51.994	9.2396×10^{-2}	-9.1517×10^{-7}	2.0658×10^{-12}	0.99944
Dimpled (d2)	61.907	0.15657	-7.9103×10^{-6}	4.4941×10^{-10}	0.99970
Dimpled (d3)	80.786	3.8592×10^{-2}	1.2851×10^{-5}	-1.3016×10^{-9}	0.99932
Dimpled (d4)	81.920	6.7621×10^{-2}	8.5542×10^{-6}	-9.2838×10^{-10}	0.99926
Dimpled (d5)	65.452	7.5728×10^{-2}	7.1629×10^{-6}	-8.2440×10^{-10}	0.99925
Offset strip fin (osf1)	57.931	0.10301	1.7997×10^{-6}	-3.6321×10^{-10}	0.99969
Offset strip fin (osf2)	57.162	8.8023×10^{-2}	1.1539×10^{-5}	-2.1143×10^{-9}	0.99841
		Heat transfer data curve fit $Nu = A + BRe + C(Re)^2 + D(Re)^3$			
Smooth (s)	6.0647	-4.3356×10^{-4}	1.0359×10^{-6}	-8.7500×10^{-11}	0.99956
Rib-roughened (r1)	3.9317	4.9271×10^{-3}	2.7681×10^{-7}	-3.8708×10^{-11}	0.99990
Rib-roughened (r2)	3.8498	4.4535×10^{-3}	6.3559×10^{-7}	-7.2915×10^{-11}	0.99989
Dimpled (d1)	2.3896	7.6226×10^{-3}	-5.0367×10^{-7}	1.9109×10^{-11}	0.99995
Dimpled (d2)	1.2416	9.6973×10^{-3}	-9.3101×10^{-7}	5.1627×10^{-11}	0.99997
Dimpled (d3)	3.2198	5.8359×10^{-3}	-1.5353×10^{-7}	-8.6982×10^{-12}	0.99995
Dimpled (d4)	1.8628	8.6480×10^{-3}	-7.3561×10^{-7}	3.8728×10^{-11}	0.99994
Dimpled (d5)	1.4229	9.7958×10^{-3}	-1.0430×10^{-6}	6.0720×10^{-11}	0.99997
Offset strip fin (osf1)	1.1631	9.5208×10^{-3}	-1.3501×10^{-6}	1.0262×10^{-10}	0.99986
Offset strip fin (osf2)	0.49902	1.0672×10^{-2}	-2.3154×10^{-6}	2.6422×10^{-10}	0.99885

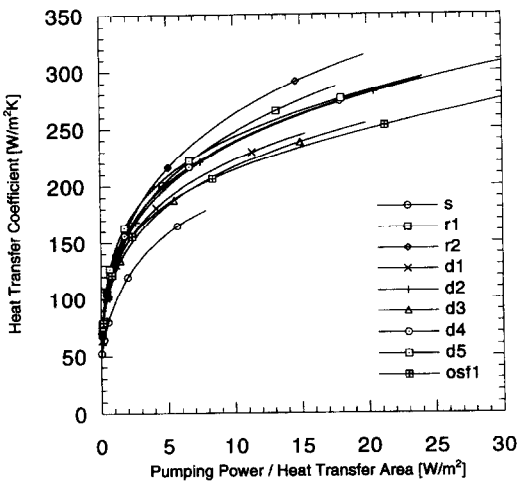

Fig. 8. The volume goodness factor.

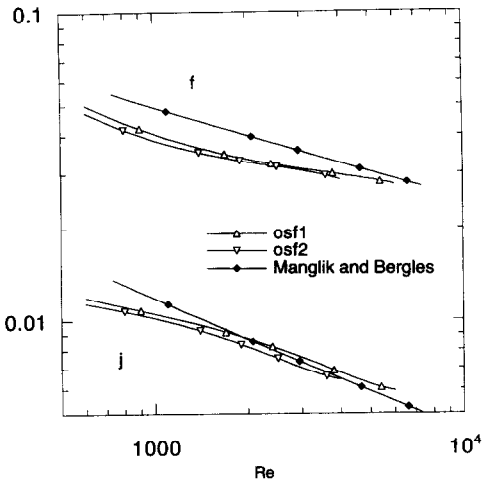

Fig. 9. Performance of offset strip fin tubes.

of caution is needed, since the volume goodness factor comparison requires equal hydraulic diameter of the tubes involved, which is not fulfilled in this case. If all tubes have $D_h = 3.11$ mm the dimpled tube d1 curve takes a higher position, while the offset strip fin tube osf1 curve comes further down in the graph. However, the ranking of the tubes remains unchanged.

The flow patterns set up by the modifications of the tubes tested are quite different. The secondary flow of a rib-roughened tube occupies the whole cross-section. Close to the walls the flow is turned sidewise due to the parallel ribs and their inclination. This motion creates an increased pressure at one side of the tube. Due to mass continuity, the flow at the central part of the tube must be in the opposite direction. Thus, the secondary flow might be a two cell swirling flow, which is effective in transporting cold fluid away from the cold walls and hot fluid from the centre of the tube towards the walls. Also, the flow pattern will most likely be influenced by the contraction in the vicinity of the ribs and the succeeding separation. This increases the turbulence intensity and improves the mixing. Metzger *et al.* [24] reported measurements in rib-roughened square channels, where in particular the effects of the rib angle were investigated. They found that the best performance was obtained when the parallel ribs had a 30° angle away from the flow and was creating a two cell secondary flow. It is expected that such a configuration will also yield favourable results in radiator tubes.

In the dimpled tubes, the flow will separate and recirculating regions may occur around the dimples. Since the dimples are closely spaced, a strong interaction of the recirculating zones appears, and locally high velocities and turbulence intensities are established. A large form drag is created and the mixing enhances the transfer of heat.

For the offset strip fin tubes, boundary layers are developed periodically in the short channels formed by the fins. However, thin wakes are also formed behind each fin. Since the fin material has a finite thickness, the flow may separate at the entrance of each channel, then reattach and develop boundary layers. The flow structure in these boundary layers may be different from conventional flat plate boundary layers. The skin friction resistance in the boundary layers and the form drag created by the wakes and the separation at the entrances are responsible for the relatively high f-factors of these tubes.

A comparison of the j and f factors for the tubes osf1 and osf2 with the correlations suggested by Manglik and Bergles [12] is found in Fig. 9. The agreement is very good between osf1 and osf2, showing that there is no influence of the tube width. The correlations of Manglik and Bergles are originally obtained with another definition of the cross-sectional area, where the fin thickness is included in the free flow width of the insert giving a lower mean velocity and thus, higher values of the j and f factors. In the present comparison the correlations are corrected for this. The difference between the measurements and the correlation is greatest at low Reynolds numbers. At $Re = 1000$ the difference is 18% in f and 11% in j. The parameters α and δ for the tubes investigated are somewhat larger than those covered by the data base of the correlations. Nevertheless, the experimental data are correlated within $\pm 20\%$.

CONCLUSIONS

The thermal and hydraulic performance of 10 radiator tubes has been investigated. The tubes tested were one smooth tube, two rib-roughened tubes, five dimpled tubes, and two offset strip fin tubes.

All the enhanced tubes provided increased heat transfer coefficients as compared to the smooth tube, but the related pressure drops were increased comparatively more than the heat transfer.

The rib-roughened tubes showed up to be the most efficient as the volume goodness factor was considered.

The offset strip fin tube data agreed within $\pm 20\%$

with the correlations available in the literature, and simple correlations were determined for $(4fRe)_{fd}$ and Nu for each tube.

Acknowledgements—This work was accomplished under the sponsorship of AB Volvo, The Swedish Board for Industrial and Technical Development (NUTEK), and Valeo Engine Cooling AB. Setrab AB provided the offset strip fin tubes.

REFERENCES

1. C. J. Davenport, *Correlations for Heat Transfer and Flow Friction Characteristics of Louvred Fins*, *AIChE Symp. Series*, No. 225, Vol. 79, 19–26 (1983).
2. A. Achaichia and T. Cowell, Heat transfer and pressure drop characteristics of flat tube and louvred plate fin surfaces, *Expl Thermal Fluid Sci.* **1**, 147–157 (1988).
3. B. Sundén and J. Svantesson, Heat transfer and pressure drop from louvered surfaces in automotive heat exchangers, *Expl Heat Transfer* **4**, 111–125 (1991).
4. B. Sundén and J. Svantesson, Heat transfer characteristics of some standard louvered surfaces for radiators. In *Heat Transfer* 1994, Vol. 6, 111–115. IChemE and Taylor and Francis (1994).
5. P. Farrell, K. Wert and R. L. Webb, Heat transfer and friction characteristics of turbulator radiator tubes, *SAE Trans.* **100,** 218–230 (1991).
6. C. O. Olsson and B. Sundén, *Hydraulic and Thermal Performance of Radiator Tubes*, Vol. VTMS-2, 1995 *Vehicle Thermal Management System*, pp. 457–462. Mechanical Engineering Publications, U.K. (1995).
7. B. H. Chang and A. F. Mills, Turbulent flow in a channel with transverse rib heat transfer augmentation. *Int. J. Heat Mass Transfer* **36,** 1459–1469 (1993).
8. Y. M. Zhang, W. Z. Gu and J. C. Han, Heat transfer and friction in rectangular channels with ribbed or ribbed-grooved walls, *ASME J. Heat Transfer* **116,** 58–65 (1994).
9. T.-M. Liou and J.-J. Hwang, Developing heat transfer and friction in a ribbed rectangular duct with flow separation at inlet, *ASME J. Heat Transfer* **114,** 565–573 (1992).
10. R. L. Webb, Enhancement of single-phase heat transfer. In *Handbook of Single-Phase Convective Heat Transfer* (Edited by S. Kakaç, R. K. Shah and W. Aung), Chap. 17, Wiley, New York (1987).
11. R. L. Webb, *Principles of Enhanced Heat Transfer*. Wiley-Interscience, New York (1994).
12. R. M. Manglik and A. E. Bergles, The thermal-hydraulic design of the rectangular offset strip fin compact heat exchanger. In *Compact Heat Exchangers* (Edited by R. K. Shah, A. D. Kraus and D. Metzger). Hemisphere, Washington, DC (1990).
13. S. Kakaç, R. K. Shah and W. Aung, *Handbook of Single-Phase Convective Heat Transfer*, Chaps 3 and 4. Wiley, New York (1987).
14. E. R. G. Eckert and R. M. Drake Jr, *Analysis of Heat and Mass Transfer*. McGraw-Hill, New York (1972).
15. W. M. Kays, Loss coefficients for abrupt changes in flow cross section with low Reynolds number flow in single and multiple tube systems. *Trans. ASME* **72,** 1067–1074 (1950).
16. W. Kays and A. L. London, *Compact Heat Exchangers*. McGraw-Hill, New York (1964).
17. R. K. Shah, Compact heat exchanger surface selection methods, *Proceedings of the Sixth International Heat Transfer Conference*, Vol. 4, 193–199 (1978).
18. T. A. Cowell, A general method for the comparison of compact heat transfer surfaces, *ASME J. Heat Transfer* **112,** 288–294 (1990).
19. G. E. P. Box, W. G. Hunter and J. S. Hunter, *Statistics for Experimenters*. Wiley, New York (1978).
20. R. J. Moffatt, Describing the uncertainties in experimental results, *Expl Thermal Fluid Sci.* **1,** 3–17 (1988).
21. R. K. Shah and A. L. London, Laminar flow forced convection in ducts. In *Advances in Heat Transfer*, Supplement 1. Academic Press, New York (1978).
22. C. O. Olsson and B. Sundén, Pressure drop characteristics of small-sized tubes, ASME-Paper 94-WA/HT-1 (1994).
23. C. O. Olsson and B. Sundén, Performance of an Automotive Heat Exchanger, *Advances in Engineering Heat Transfer* (Edited by B. Sundén, E. Blums and A. Zukauskas), pp. 309–319. Computational Mechanics Publications, Southampton (1995).
24. D. E. Metzger, C. S. Fan and Y. Yu, Effects of rib angle and orientation on local heat transfer in square channels with angled roughness ribs. In *Compact Heat Exchangers* (Edited by R. K. Shah, A. D. Kraus and D. Metzger). Hemisphere, Washington, DC (1990).